Repair of O^6-G-Alkyl-O^6-G Interstrand Cross-Links by Human O^6-Alkylguanine-DNA Alkyltransferase†

Qingming Fang,‡ Anne M. Noronha,§ Sebastian P. Murphy,§ Christopher J. Wilds,§ Julie L. Tubbs,|| John A. Tainer,|| Goutam Chowdhury,⊥ F. Peter Guengerich,⊥ and Anthony E. Pegg*,‡

Departments of Cellular and Molecular Physiology and Pharmacology, The Pennsylvania State University College of Medicine, P.O. Box 850, Hershey, Pennsylvania 17033, Department of Chemistry and Biochemistry, Concordia University, 7141 Sherbrooke Street West, Montreal, QC, Canada H4B 1R6, The Skaggs Institute for Chemical Biology and Department of Molecular Biology, The Scripps Research Institute, 10550 North Torrey Pines Road, MB4, La Jolla, California 92037, and Department of Biochemistry and Center in Molecular Toxicology, Vanderbilt University School of Medicine, Nashville, Tennessee 37232

Received May 12, 2008; Revised Manuscript Received July 11, 2008

ABSTRACT: O^6-Alkylguanine-DNA alkyltransferase (AGT) plays an important role by protecting cells from alkylating agents. This reduces the frequency of carcinogenesis and mutagenesis initiated by such agents, but AGT also provides a major resistance mechanism to some chemotherapeutic drugs. To improve our understanding of the AGT-mediated repair reaction and our understanding of the spectrum of repairable damage, we have studied the ability of AGT to repair interstrand cross-link DNA damage where the two DNA strands are joined via the guanine-O^6 in each strand. An oligodeoxyribonucleotide containing a heptane cross-link was repaired with initial formation of an AGT−oligo complex and further reaction of a second AGT molecule yielding a hAGT dimer and free oligo. However, an oligodeoxyribonucleotide with a butane cross-link was a very poor substrate for AGT-mediated repair, and only the first reaction that forms an AGT−oligo complex could be detected. Models of the reaction of these substrates in the AGT active site show that the DNA duplex is forced apart locally to repair the first guanine. This reaction is greatly hindered with the butane cross-link, which is mostly buried in the active site pocket and limited in conformational flexibility. This limitation also prevents the adoption of a conformation for the second reaction to repair the AGT−oligo complex. These results are consistent with the postulated mechanism of AGT repair that involves DNA binding and flipping of the substrate nucleotide and indicate that hAGT can repair some types of interstrand cross-link damage.

O^6-Alkylguanine-DNA alkyltransferase (AGT)[1] is a widely distributed DNA repair protein for the maintenance of genomic integrity (*1*−*4*). It acts on adducts at the O^6-position of guanine and transfers the alkyl group to an internal Cys residue, restoring the DNA in a single step. The *S*-alkyl-Cys formed is not regenerated, and the protein can act only once. Human O^6-alkylguanine-DNA alkyltransferase (hAGT) can repair not only methyl groups but also longer alkyl groups, including ethyl, 2-chloroethyl, and butyl groups, and more bulky cyclic adducts such as benzyl and pyridyloxobutyl groups (*5*−*7*). In addition to the beneficial effects of protection from carcinogens and mutagens such as *N*-methyl-*N*′-nitro-*N*-nitrosoguanidine, dimethylnitrosamine, *N*-ethyl-*N*-nitrosourea, methylbenzylnitrosamine, and 4-(methylnitrosamino)-1-(3-pyridyl)-1-butanone, hAGT has the deleterious effect of providing resistance to killing of cancer cells by therapeutic alkylating drugs such as the methylating agent Temozolomide and the chloroethylating agent 1,3-bis(2-chloroethyl)-1-nitrosourea (*8*).

The resistance to such chloroethylating agents is caused by the efficient repair of O^6-chloroethylguanine adducts. This prevents the formation of the primary toxic lesion, which is a 1-(3-cytosinyl)-2-(1-guanyl)ethane interstrand cross-link (*9, 10*). This is formed spontaneously in a two-step process from the O^6-(2-chloroethyl)guanine that undergoes an internal cyclization to form 1,O^6-ethanoguanine which, in turn, reacts with the opposite strand cytosine to yield the interstrand cross-link (*11, 12*). The final cross-link does not involve the

† This research was supported by Grants CA-018137 (A.E.P.), CA-097209 (J.A.T.), and R01 ES10546 and P30 ES000267 (F.P.G.) from the U.S. Public Health Service and by funding from the Natural Sciences and Engineering Research Council of Canada (NSERC), the Canada Foundation for Innovation (CFI), and the Canada Research Chair (CRC) program. We also acknowledge a Merck Fellowship for financial support (G.C.).

* To whom correspondence should be addressed: Department of Cellular and Molecular Physiology, Pennsylvania State University College of Medicine, The Milton S. Hershey Medical Center, P.O. Box 850, 500 University Dr., Hershey, PA 17033. Telephone: (717) 531-8152. Fax: (717) 531-5157. E-mail: aep1@psu.edu.

‡ Pennsylvania State University College of Medicine.

§ Concordia University.

|| The Scripps Research Institute.

⊥ Vanderbilt University School of Medicine.

[1] Abbreviations: AGT, O^6-alkylguanine-DNA alkyltransferase; hAGT, human AGT; busulfan, 1,4-butanediol dimethanesulfonate; hepsulfam, 1,7-heptanediol disulfamate; oligo, oligodeoxyribonucleotide; IPTG, isopropyl β-D-thiogalactopyranoside; PNK, T4 polynucleotide kinase; DTT, dithiothreitol; SDS−PAGE, sodium dodecyl sulfate−polyacrylamide gel electrophoresis; DBE, 1,2-dibromoethane; MS, mass spectrometry; TFA, trifluoroacetic acid; MP, median product of the repair reaction (hAGT−oligo); FP, final product of the repair reaction (free oligo).

10.1021/bi8008664 CCC: $40.75
Published on Web 09/20/2008

O^6-position of guanine and is unaffected by AGT. However, it was shown that the intermediate 1,O^6-ethanoguanine was a substrate for AGT, and its repair leads to a DNA−protein cross-link in which the AGT is joined by an ethano linkage to N1 of guanine (*13, 14*). Structural and biochemical studies of the repair reaction brought about by hAGT have provided a plausible preliminary model for understanding the mechanism of DNA repair (*4, 15*−*19*). Available crystal structures of human hAGT include those with the inactive C145S mutant bound to DNA containing O^6-methylguanine (*16*), wild-type AGT cross-linked to the mechanistic inhibitor N1,O^6-ethanoxanthosine (*16*), and wild-type protein bound to a DNA containing a modified cytosine residue (*17*). These structures indicate that hAGT binds substrate DNA via the minor groove using a helix−turn−helix motif. The alkylated guanine deoxynucleotide is flipped out from the base stack into the AGT active site pocket via a 3′-phosphate rotation, which is promoted by Tyr114, either by steric (*16*) or by electrostatic effects (*19*), and stabilized by an Arg finger (Arg128). An asparagine hinge formed by Asn137 couples the helix−turn−helix DNA binding and active site motifs. The extruded O^6-alkylguanine is positioned for repair in a hydrophobic cleft made up of the Met134 side chain and Val155−Gly160 of the active site loop. Cys145 and Val148 carbonyls accept hydrogen bonds from guanine's exocyclic amine, and Tyr114 hydroxyl and Ser159 N atoms donate hydrogen bonds to guanine's N3 and O^6 atoms, respectively. These interactions position the alkyl group for attack by Cys145, which has a very high reactivity (*20*) due to its activation to a thiolate anion by a Glu172−His146−water−Cys145 hydrogen bond network (*4, 15*). The reaction may also be facilitated by reduction of the negative charge on the repaired guanine via the hydrogen bond from Tyr114. The description given above (and amino acid numbering) relates to the hAGT, but it is likely to be universally applicable since all of the key residues mentioned above are highly conserved and the structures of three other AGTs from the bacterium *Escherichia coli* (Ada-C) (*21*), the archaebacterium *Pyrococcus kodakaraensis* (*22*), and the thermophile *Methanococcus jannaschii* (*23*) are generally similar, particularly in the active site and DNA binding domains. Further details of the mechanism by which lesions are identified and the DNA structure is altered to allow repair by AGTs remain to be identified.

In the experiments presented here, we have examined the repair of DNA interstrand cross-links formed between the O^6-position of two guanine residues. These experiments had two aims: (1) to establish whether the repair of such cross-links that may be formed by bifunctional agents such as 1,4-butanediol dimethanesulfonate (busulfan) and 1,7-heptanediol disulfamate (hepsulfam), which are developmental anticancer agents (*24, 25*), could influence response to these drugs and (2) to obtain more information about the AGT-mediated repair of structurally restricted substrates. Studies were carried out with oligodeoxyribonucleotide (oligo) substrates containing alkyl cross-links with seven carbons and four carbons and using wild-type hAGT and mutants at key active site residues and with *E. coli* AGTs. It was found that the human but not *E. coli* AGTs were competent to repair the longer cross-link but that the shorter cross-link was highly resistant to repair. Modeling studies based on the crystal structure of hAGT and Ada-C provide a plausible explanation for these results, and further support was generated from the results of studies with mutants of hAGT at positions Arg128 and Tyr114.

Table 1: Sequences and Structures of Oligodeoxyribonucleotides Used[a]

Oligodeoxyribonucleotide	Nucleotide Sequence
CJW80	5'-CGAAA**X**^{7}TTTCG-3' 3'-GCTTT**X**^{7}AAAGC-5'
80-C	5-CGAAAGTTTCG-3'
CJW81	5'-CGAA**X**^{7}CTTCG-3' 3'-GCTTC**X**^{7}AAGC-5'
81-C	5'-CGAAGCTTCG-3'
CJW98	5'-CGACTAAA**X**^{7}TTTAGTCG-3' 3'-GCTGATTT**X**^{7}AAATCAGC-5'
98-C	5'-CGACTAAAGTTTAGTCG-3'
CJW119	5'-CGAAA**X**^{4}TTTCG-3' 3'-GCTTT**X**^{4}AAAGC-5'

[a] The structures of $\underline{\mathbf{X}}^7$ and $\underline{\mathbf{X}}^4$ are shown in Figure 1.

EXPERIMENTAL PROCEDURES

Materials. All the control unmodified oligos were synthesized and purified by the Macromolecular Core Facility, Hershey Medical Center. Ampicillin, isopropyl β-D-thiogalactopyranoside (IPTG), hemocyanin, calf thymus DNA, and most other biochemical reagents were purchased from Sigma Chemical Co. (St. Louis, MO). Talon Metal Affinity IMAC Resin was obtained from BD Bioscience Clontech (Palo Alto, CA); liquid acrylamide/bisacrylamide (37.5:1) and urea were purchased from Roche Diagnostic Corp. (Indianapolis, IN). Nitrocellulose filters (0.45 μm) were obtained from Millipore. PVDF membrane was purchased from Pall Life Sciences (Pensacola, FL). T4 polynucleotide kinase (PNK) was purchased from New England Biolabs (Beverly, MA). [γ-^{35}S]ATPγS was purchased from Amersham (Piscataway, NJ). Sequence grade modified trypsin was obtained from Promega (Madison, WI). Tobacco etch virus (Tev) protease (*26*) was generously provided by J. M. Flanagan (Department of Biochemistry and Molecular Biology, Penn State University, University Park, PA). Penta His antibody was obtained from Qiagen (Chatsworth, CA). HRP-linked anti-mouse IgG, anti-rabbit IgG, and lumiGLO reagent were purchased from Cell Signal Technology (Danvers, MA).

Cross-Linked Oligonucleotide Preparation and Purification. The oligos that were used are listed in Table 1, and the structure of the cross-link is shown in Figure 1. Studies were carried out with double-stranded 10 bp substrate (CJW81), 11 bp substrates (CJW80 and CJW119), and the 17 bp CJW98. The CJW119 substrate contained a butane cross-link, and the CJW80, CJW81, and CJW98 substrates contained a heptane cross-link. The linked guanine residues were opposite one another in all substrates except CJW81,

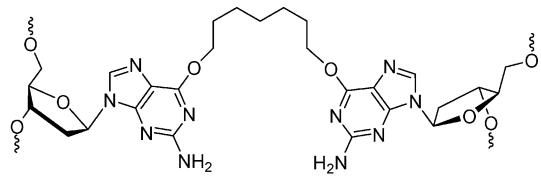

X^7

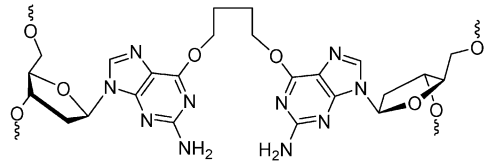

X^4

FIGURE 1: Structures of cross-links.

where the linked guanines were paired with a cytosine in the opposite strand.

Cross-linked phosphoramidite dimers containing butyl and heptyl linkers were synthesized and the oligo substrates prepared by solid phase synthesis using an ABI 3400 oligonucleotide synthesizer and purified as described below. 5′-*O*-Dimethoxytrityldeoxyribonucleoside-3′-*O*-(*β*-cyanoethyl-*N*,*N*′-diisopropyl) phosphoramidites and controlled pore glass (CPG) supports (500 Å) derivatized with protected 2′-deoxynucleosides were purchased from ChemGenes Inc. (Wilmington, MA). Bis-3′-*O*-phosphoramidites containing four- and seven-carbon linkers between the O^6 atoms of two 2′-deoxyguanosines were synthesized from N^2-phenoxyacetyl-2′-deoxyguanosine according to published procedures (*27*). The cross-linked duplexes CJW80, -81, -98, and -119 were assembled on an Applied Biosystems model 3400 synthesizer on a 1 *μ*mol synthesis scale using standard *β*-cyanoethylphosphoramidite chemistry. The nucleoside phosphoramidites were dissolved in anhydrous acetonitrile at a concentration of 0.1 M for the 3′-*O*-deoxyphosphoramidites and 0.05 M for the cross-linked bis-3′-*O*-deoxyphosphoramidites. Assembly of the sequences was carried out as follows: (a) detritylation, 3% trichloroacetic acid in dichloromethane; (b) nucleoside phosphoramidite coupling for 2 min for commercial 3′-*O*-deoxyphosphoramidites and 30 min for the cross-linked bis-phosphoramidites; (c) capping, 1:1:8 (v/v/v) phenoxyacetic anhydride/pyridine/tetrahydrofuran mixture (solution A) and 16:84 (w/v) 1-methyl-1*H*-imidazole/tetrahydrofuran mixture (solution B); (d) oxidation, 0.02 M iodine in a 2.5:2:1 tetrahydrofuran/water/pyridine mixture. The 5′-*O*-terminal trityl groups were removed on the synthesizer.

The oligomer-derivatized supports were transferred to screw cap microfuge tubes lined with Teflon caps and the protecting groups removed with a concentrated ammonium hydroxide (0.3 mL)/ethanol (0.1 mL) treatment for 4 h at 55 °C. The oligomers were then purified by SAX HPLC using a Dionex DNAPAC PA-100 column (0.4 cm × 25 cm; Dionex Corp., Sunnyvale, CA) with a linear gradient from 0 to 50% buffer B over 30 min [where buffer A consisted of 0.1 M Tris-HCl (pH 7.5) and 10% acetonitrile and buffer B consisted of 0.1 M Tris-HCl (pH 7.5), 1 M NaCl, and 10% acetonitrile] at 30 °C. The detector was set at 260 nm for analytical runs and 290 nm for preparative runs. The purified oligomers were desalted using C-18 SEP PAK cartridges (Waters Inc.).

The cross-linked oligomers (0.1 A_{260} unit) were characterized by digestion with a combination of snake venom phosphodiesterase (0.28 unit) and calf intestinal phosphatase (5 units) in a buffer containing 10 mM Tris (pH 8.1) and 2 mM magnesium chloride for 16 h at 37 °C. The resulting mixture of nucleosides was analyzed by reversed phase HPLC carried out using a Symmetry C-18 5 *μ*m column (0.46 cm × 15 cm) purchased from Waters Inc. (Milford, MA). The C-18 column was eluted with a linear gradient from 0 to 60% buffer B over 30 min [where buffer A consisted of 50 mM sodium phosphate (pH 5.8) and buffer B consisted of 50 mM sodium phosphate (pH 5.8) and 50% acetonitrile]. The resulting peaks were identified by coinjection with the corresponding standards, and the ratio of nucleosides was determined. The molecular weights of the cross-linked oligomers were determined by ESI-MS, and these were in agreement with the calculated values.

Protein Purification. Plasmids for the production of N-terminally His_6-tagged hAGT, N-terminally His_6-tagged hAGT mutants R128K, R128A, R128G, C145A, P140K, Y158H, and G160R, and *E. coli* Ogt; C-terminally His_6-tagged hAGT and C-terminally His_6-tagged hAGT mutants Y114F, Y114A, and C145S, and *E. coli* Ada-C; and Tev-hAGT with a Tev protease cleavable His_6 tag were prepared as described previously (*28*−*32*). Studies with wild-type hAGT showed that the presence or positioning of the His_6 tag did not affect the results. Proteins were expressed in XL-1 blue cells and purified using Talon IMAC resin. To remove the His_6 tag from Tev-hAGT, the protein was dialyzed in 50 mM Tris-HCl (pH 7.6), 1 mM dithiothreitol (DTT), and 0.1 mM EDTA and then concentrated to <1.0 mL with a Centrion Ultracel YM-10 apparatus from Millipore Corp. (Bedford, MA) before digestion by Tev protease (1:20 ratio) as described previously (*26, 32*). The purified protein was analyzed by SDS−PAGE on 12% gels.

Alkyltransferase Activity Assays. The purified AGT proteins were assayed by measuring the ability of the protein to transfer methyl groups from a ^{3}H-labeled methylated DNA substrate as previously described (*29, 32*). The protein was incubated with 10 *μ*g of ^{3}H-labeled methylated DNA substrate in 1.0 mL of 50 mM Tris-HCl buffer (pH 7.6) containing 5 mM DTT, 0.1 mM EDTA (AGT buffer), and 50 *μ*g of hemocyanin for 2 h at 37 °C; 0−2.5 pmol of hAGT, Ogt, Ada-C, G160R, or R128K, 0−9 pmol of Y114F, P140K, or Y158H, 0−700 pmol of R128A, R128G, or Y114A was used in the assay. Nitrocellulose filters were used to collect the formed ^{3}H-labeled methylated protein and counted in scintillation liquid. At the counting efficiency that was used, 1 fmol of transferred methyl groups was equal to 20 cpm.

Polyacrylamide Gel Electrophoresis Assay of O^6-G-Alkyl-O^6-G Interstrand Cross-Link Repair. The cross-link-containing oligos, CJW80, CJW81, CJW98, and CJW119, and corresponding controls were labeled at the 5′-end with [*γ*-^{35}S]ATP*γ*S. Labeling was carried out in 50 *μ*L of reaction buffer composed of 1× T4 PNK buffer (New England Biolabs), 4 *μ*L of [*γ*-^{35}S]ATP*γ*S (10 *μ*Ci/*μ*L), 10 units of T4 PNK, and 500 pmol of oligo. The mixture was incubated at 37 °C for 1 h, and then the reaction was stopped by heating the mixture at 65 °C for 20 min. The labeled oligos were passed through a Sephadex MicroSpin G-25 column to remove unincorporated [*γ*-^{35}S]ATP*γ*S. The purified and

labeled oligos were heated to 100 °C and allowed to cool to room temperature.

The repair of these substrates was studied by incubation with the AGT protein as indicated (0−60 pmol) in 15 μL of AGT buffer with the labeled substrate oligo (2−4 pmol) for up to 2 h at 37 °C. The products of the reaction were then analyzed either by sodium dodecyl sulfate−polyacrylamide gel electrophoresis (SDS−PAGE) or by denaturing PAGE in 7 M urea (*33*). For analysis by SDS−PAGE, the reaction was terminated by the addition of 10 μL of loading buffer [containing 125 mM Tris-HCl (pH 7.6), 5% SDS, and 25% glycerol (v/v)] and the samples were loaded on 20% mini-SDS−PAGE gels with 0.125 M Tris-HCl buffer containing 0.1% SDS and run for 60−80 min with a voltage of 100−120 V. The gels were fixed, dried, and quantified on a Molecular Dynamics PhosphorImager SI system (Molecular Dynamics, Mountain View, CA) using ImageQuant (Amersham Biosciences). The band of each lane on the gel representing different products or substrate was quantitated and calculated using the control band as a reference. A control of AGT covalently linked to an oligo by reaction with 1,2-dibromoethane (DBE) was prepared by incubation of 60 pmol of hAGT and 4 pmol of oligo with 300 pmol of DBE in 15 μL for 2 h (*34*) and loaded onto the gels.

For analysis by denaturing PAGE (*33*), the samples were prepared as described above but the reaction was stopped by the addition of 1.6 μL of 10% SDS and 16.6 μL of loading buffer containing 80% formamide in 1× TBE [89 mM Tris-HCl, 89 mM boric acid, and 2 mM EDTA (pH 8.0)] buffer. Samples were heated for 5 min in boiling water and loaded onto 17% 18 cm × 16 cm polyacrylamide gels with 7 M urea in 1× TBE buffer and run for 3−4 h with a voltage of 200−250 V. The gels were treated and the products quantitated as described above.

Detection of the DNA−AGT(peptide) Cross-Link Product by Mass Spectrometry (MS). hAGT (400−600 pmol, N-His-tagged or C-His-tagged) was incubated with CJW98 (200 pmol) in 15 μL of AGT reaction buffer for 3 h at 37 °C. Reactions were terminated by the addition of 10 μL of loading buffer [containing 125 mM Tris-HCl (pH 7.6), 2% SDS, and 25% glycerol]. Samples were subsequently heated at 100 °C for 5 min and separated on 20% mini-SDS−PAGE gels with 0.125 M Tris-HCl and 0.1% SDS and run for 60−80 min with a voltage of 100−120 V. Gel slices containing the Coomassie blue-stained bands corresponding to the hAGT bound to the oligo were excised, washed with 50% acetonitrile containing 0.1% trifluoroacetic acid (TFA), destained twice with 200 μL of 100 mM ammonium bicarbonate (pH 8.0) and 50% acetonitrile for 45 min at 37 °C, and dried in a SpeedVac. The gel slices were then incubated with 0.02 μg/μL trypsin in digestion buffer (1.5 times the volume of the original gel slice) containing 10% acetonitrile, 40 mM NH_4HCO_3 (pH 8.0), 0.1% (w/v) *n*-octyl glucoside, and 0.1% TFA for 1 h at room temperature. The buffer was removed, and an additional 100−200 μL of digestion buffer was added and incubated for 4−5 h at 48 °C. The solution was removed and kept in a new prewashed tube. After addition of 100 μL of 0.1% TFA to the gel slice, it was incubated for an additional 1 h at 37 °C. The solution was removed and added to the first extraction. The combined sample was then dried and resuspended in 200 μL of water three times to remove volatile materials. A final volume of ∼10 μL was used for analysis.

Samples were analyzed in an ESI linear trap ion mass spectrometer (LTQ, Thermo-Fisher, San Jose, CA) connected to a Waters Acquity UPLC system using an Aquity UPLC BEH C18 column (1.7 μm, 1.0 mm × 100 mm). DNA−peptide cross-links were separated using buffer A containing 10 mM $NH_4CH_3CO_2$ and 2% CH_3CN (v/v) and buffer B containing 10 mM $NH_4CH_3CO_2$ and 95% CH_3CN (v/v) following a gradient program with a flow rate of 150 μL/min: from 0 to 3.0 min, linear gradient from 100 to 97% A; from 3.0 to 6.0 min, linear gradient to 80% A; from 6.0 to 6.5 min, linear gradient to 100% B; from 6.5 to 8.5 min, hold at 100% B; from 8.5 to 9.0 min, linear gradient to 100% A; from 9.0 to 12.0 min, hold at 100% A. The temperature of the column was maintained at 50 °C, and samples (10 μL) were infused with an autosampler. ESI conditions were as follows: source voltage, 4 kV; source current, 100 μA; auxiliary gas flow rate setting, 20; sweep gas flow rate setting, 5; sheath gas flow setting, 34; capillary voltage, −49 V; capillary temperature, 350 °C; tube lens voltage, −90 V. MS/MS conditions were as follows: normalized collision energy, 35%; activation *Q*, 0.250; activation time, 30 ms. The quadruply charged species (*m*/*z* 1653.8) were used for CID analysis. The *m*/*z* values of the CID fragments corresponding to the peptide−DNA cross-link were calculated using a program linked to the Mass Spectrometry Group of Medicinal Chemistry at the University of Utah (medlib.med.utah.edu/masspec/).

Western Blot Analysis. To detect the cross-linked AGT dimer, hAGT was incubated with potential substrate oligos (unlabeled) in AGT buffer for up to 2 h at 37 °C and the reaction was terminated by the addition of loading buffer containing 2% SDS. The samples were heated at 100 °C for 5 min, separated by 15% SDS−PAGE, and electrotransferred to PVDF membranes. Detection was carried out using ATO-1 antibody (*35*), which is a polyclonal antiserum raised in rabbits to a peptide corresponding to residues Lys8−Glu20, or anti-Penta His antibody, which recognizes the His_6 tag as the primary antibody and HRP-linked anti-rabbit IgG or anti-mouse IgG as the secondary antibody and the chemiluminescent reagent lumiGLO used to visualize the immunoreactive bands.

Generation of Models for Alkyl Interstrand Cross-Link Repair by hAGT. Initial models of oligonucleotides containing alkyl interstrand cross-links with four or seven carbons were built and manually placed in the hAGT active site (PDB entry 1t38), using AGT crystal structures (PDB entries 1eh6, 1eh8, and 1t39) as guides for DNA and Cys145 side chain placement. Initial models were subjected to conjugate gradient minimization, simulated annealing, and torsion angle dynamics by Crystallography & NMR System (CNS) (*36*), which employs molecular dynamics with CHARMM (Chemistry at HARvard Macromolecular Mechanics) (*37, 38*) force field parameters. One hundred steps of conjugate gradient minimization were followed by 40 steps of simulated annealing. Simulated annealing was carried out at a starting temperature of 1000 K and slow cooling with a drop in temperature of 25 K per cycle of dynamics. Human AGT (PDB entry 1t38) active site analysis was conducted with the CASTp (*39*) (http://sts-fw.bioengr.uic.edu/castp/index.php) and MOLEOnline (*40*) (http://mole.chemi.muni.cz/

index.php) servers. The models were validated using the rigorous structure validation programs ProCheck, WhatCheck, Errat, and Prove of the JCSG Protein Structure Validation Suite (http://www.jcsg.org/prod/scripts/validation/sv3.cgi), the Verify3D Structure Evaluation Server (http://nihserver.mbi.ucla.edu/Verify_3D), and MolProbity (http://molprobity.biochem.duke.edu). These programs, which are routinely used for checking quality of models in theoretical studies, indicated that models for four- and seven-carbon alkyl interstrand cross-link repair by hAGT were acceptable and comparable to PDB entry 1t38 from which they were derived.

RESULTS

Repair of an Alkyl Interstrand Cross-Link with Seven Carbons by hAGT. The labeled double-stranded 11-mer substrate CJW80 was incubated with hAGT, and the products were identified via SDS−PAGE (Figure 2A). As one can see by comparing lanes 1 and 2 with lane 4, the incubation with wild-type hAGT led to a loss of the substrate oligo and the appearance of two new product bands. A larger amount of the substrate was converted when the amount of hAGT added was increased (lanes 7 and 8). These product bands were not formed when hAGT that had been inactivated with SDS (lane 10) or the C145S mutant (lane 9) was used, showing that active AGT was needed. The most rapidly migrating product band corresponds to the free oligo marker 80-C (lane 3). The more slowly migrating band corresponds approximately to the lower band of a marker in which the labeled oligo was covalently attached to AGT by reaction with DBE (lanes 5 and 6). Previous studies in which this reaction was fully characterized (*34, 41*) show that the adduct is formed by an ethane bridge between the Cys145 side chain of hAGT and the N7 or N^2 position of a guanine residue in the added oligo. Multiple hAGT molecules can be added to an oligo containing multiple guanine residues in this reaction, and the upper band in this marker is likely to represent the attachment of two AGT molecules. The very slight difference in the mobility of the product of the repair of CJW80 by AGT and the lower marker band formed by DBE is likely to be due to either the longer alkane bridge or the fact that the hAGT−oligo cross-link formed in the repair reaction would be expected to be attached at the O^6-position of guanine.

These experiments indicate that the cross-link of CJW80 and CJW98 could be repaired by hAGT and forms a hAGT−DNA complex (median product, MP) and free oligo (final product, FP) (Figures 2 and 3). As both strands of CJW80 were 5′-end-labeled, if only one side of the alkyl cross-link were repaired, the ratio of MP to FP-1 would be close to 1. However, the yield of free oligo was much more than that of the MP (Figure 2C), suggesting that both sides of cross-link are efficiently repaired by hAGT. Essentially the same results were obtained when the products of the reaction with CJW80 were analyzed using gels that contained 7 M urea (denaturing PAGE) (Figure 2B), but in this case, the amount of FP was increased slightly and the amount of MP decreased (Figure 2C). This difference is likely to be due to the formation of a doubly stranded product after the cross-link is repaired. If the released strand is not dissociated from the hAGT−oligo MP, radioactivity that should be associated with the FP will remain with the MP. The

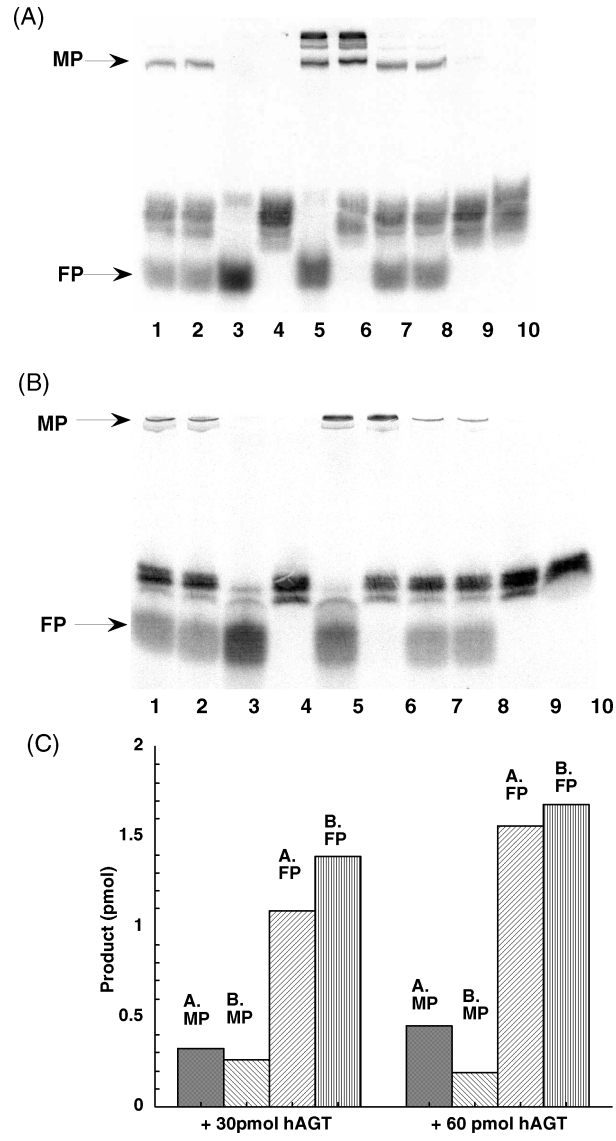

FIGURE 2: Repair of 11-mer seven-carbon cross-linked oligo CJW80 by hAGT. (A) Oligos were incubated with hAGT at 37 °C for 2 h, and the products were separated via SDS−PAGE as described in Experimental Procedures: lanes 1 and 2, 4 pmol of CJW80 and 30 pmol of hAGT; lane 3, 4 pmol of 80-C (FP marker); lane 4, 4 pmol of CJW80; lane 5, 4 pmol of 80-C, 60 pmol of hAGT, and 300 pmol of DBE (MP marker); lane 6, 4 pmol of CJW80, 60 pmol of hAGT, and 300 pmol of DBE (MP marker); lanes 7 and 8, 4 pmol of CJW80 and 60 pmol of hAGT; lane 9, 4 pmol of CJW80 and 60 pmol of C145S; lane 10, 4 pmol of CJW80 and 60 pmol of inactivated hAGT (hAGT inactivated by SDS). (B) The products were separated by denaturing PAGE as described in Experimental Procedures. Lanes as in panel A. (C) The amount of products was determined with ImageQuant, and the amount of product formed is shown: MP, hAGT−DNA complex; FP, free 11-mer oligo.

denaturing PAGE conditions provide a more complete dissociation of the complex. However, the resolution in the area of the gel occupied by the hAGT−DNA complex is better under the SDS−PAGE conditions (compare MP in panels A and B of Figure 2).

These results were confirmed by studies in which the labeled double-stranded 17-mer substrate CJW98 was incubated with hAGT (Figure 4). Irrespective of whether the products were separated by SDS−PAGE (Figure 4A) or denaturing PAGE (Figure 4B), there was clear formation of a FP corresponding to the single-stranded 17-mer and an intermediate product corresponding to the hAGT−oligo

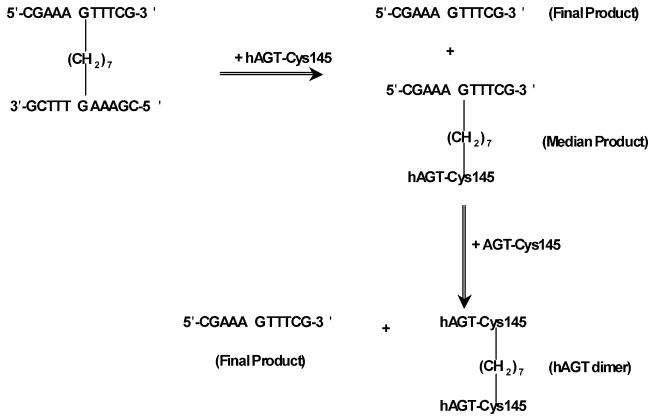

FIGURE 3: Repair of cross-links by hAGT. The scheme is shown with an 11-mer substrate such as CJW80, but similar reactions would occur with 17-mer substrate CJW98 and 10-mer substrate CJW81.

complex. Quantification of these results is shown in Figure 4C. There was a greater discrepancy between the relative amounts of MP and FP assayed under SDS−PAGE and denaturing PAGE conditions with the 17-mer cross-linked substrate compared to the results with 11-mer cross-linked substrate shown in Figure 2. The amount of the AGT−oligo complex (MP) found was substantially reduced when separated by denaturing PAGE, and there was a corresponding increase in the amount of free 17-mer FP (Figure 4C). This result is consistent with the explanation given above since the repaired 17-mer strand is less likely to dissociate from the AGT−oligo complex than the 11-mer product under the SDS−PAGE conditions.

The identity of the MP formed in the reaction with CJW98 was confirmed by LC−MS analysis. After separation by SDS−PAGE, the band corresponding to the AGT−oligo complex (MP) was eluted from the gel and digested with trypsin. The digest was analyzed by LC−MS (Figure 5 and Supporting Information Table S1) which confirmed the presence of a peptide corresponding to the oligo linked via a $(CH_2)_7$ moiety to a peptide derived from residues Gly136−Arg147 of hAGT which contains the Cys145 acceptor site.

A time course of the repair of the double-stranded 17-mer substrate CJW98 by hAGT with analysis carried out using the denaturing PAGE conditions is shown in Figure 6. The production of the free 17-mer FP continued to increase with time over a 2 h incubation, whereas the hAGT−oligo MP peaked at ~45 min. The ratio of MP to FP continuously declined from a maximum at 5 min. This experiment supports the interpretation that both O^6-adducts in the substrate could efficiently be repaired with initial formation of an hAGT−oligo complex and further reaction yielding a hAGT dimer and free oligo.

The formation of an hAGT dimer was confirmed by Western blotting analysis shown in Figure 7. After incubation of active hAGT with CJW98 and separation of the products by SDS−PAGE, a band of ~44 kDa was produced that reacts with an antibody to hAGT (lanes 1−5 in Figure 7). The MP with hAGT linked to the 17-mer (~23.7 kDa) can also be seen just above the band corresponding to the hAGT monomer (~22 kDa).

Oligos CJW98 and CJW80 contain a seven-carbon alkyl interstrand cross-link between two opposing guanine resi-

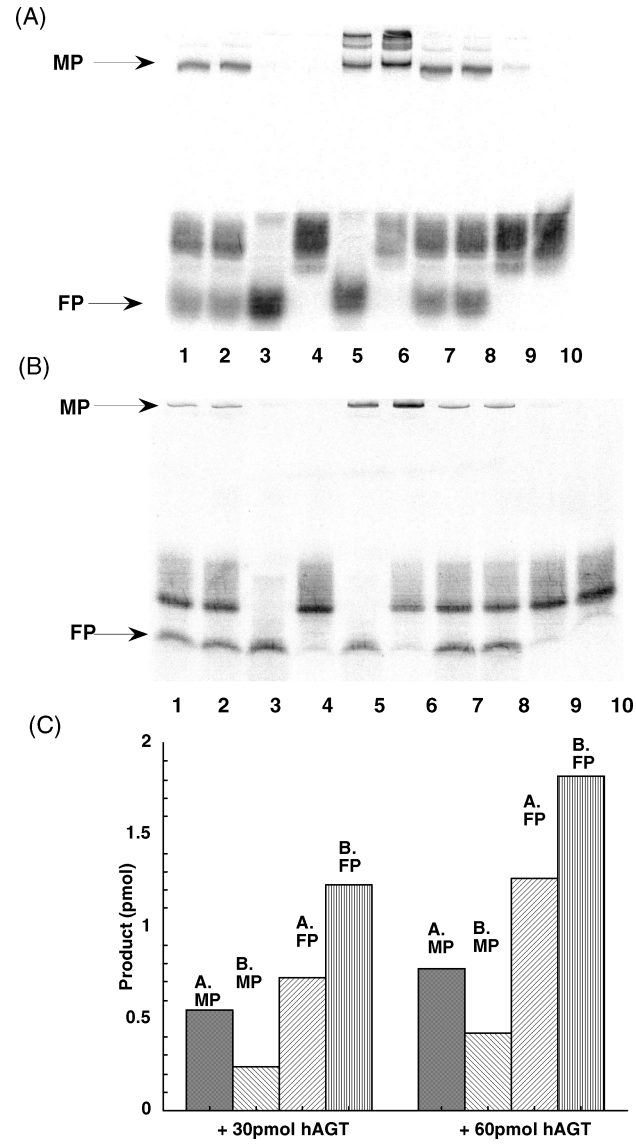

FIGURE 4: Repair of 17-mer seven-carbon cross-linked oligo CJW98 by hAGT. (A) Oligos were incubated with hAGT at 37 °C for 2 h, and the products were separated by SDS−PAGE as described in Experimental Procedures: lanes 1 and 2, 4 pmol of CJW98 and 30 pmol of hAGT; lane 3, 4 pmol of 98-C (FP marker); lane 4, 4 pmol of CJW98; lane 5, 4 pmol of 98-C, 60 pmol of hAGT, and 300 pmol of DBE (MP marker); lane 6, 4 pmol of CJW98, 60 pmol of hAGT, and 300 pmol of DBE (MP marker); lanes 7 and 8, 4 pmol of CJW98 and 60 pmol of hAGT; lane 9, 4 pmol of CJW98 and 60 pmol of C145S; lane 10, 4 pmol of CJW98 and 60 pmol of inactivated hAGT (hAGT inactivated by SDS). (B) The products were separated by denaturing PAGE as described in Experimental Procedures. Lanes as in panel A. (C) The amount of products was determined with ImageQuant, and the amount of product formed is shown: MP, hAGT−DNA complex; FP, free 17-mer oligo.

dues, which would not normally be paired in a double-stranded DNA. However, the possible distortion associated with this linkage is not a critical factor in allowing repair since oligo CJW81 (Figure 1), which is a 10-mer oligo containing a central seven-carbon alkyl interstrand cross-link in which the cross-linked guanines are paired with cytosine, was also repaired well by hAGT. The rate of repair of this oligo was only slightly lower than that of CJW80 or CJW98 (Figure 8).

Repair of an Alkyl Interstrand Cross-Link with Four Carbons by hAGT. In contrast to the efficient repair of the

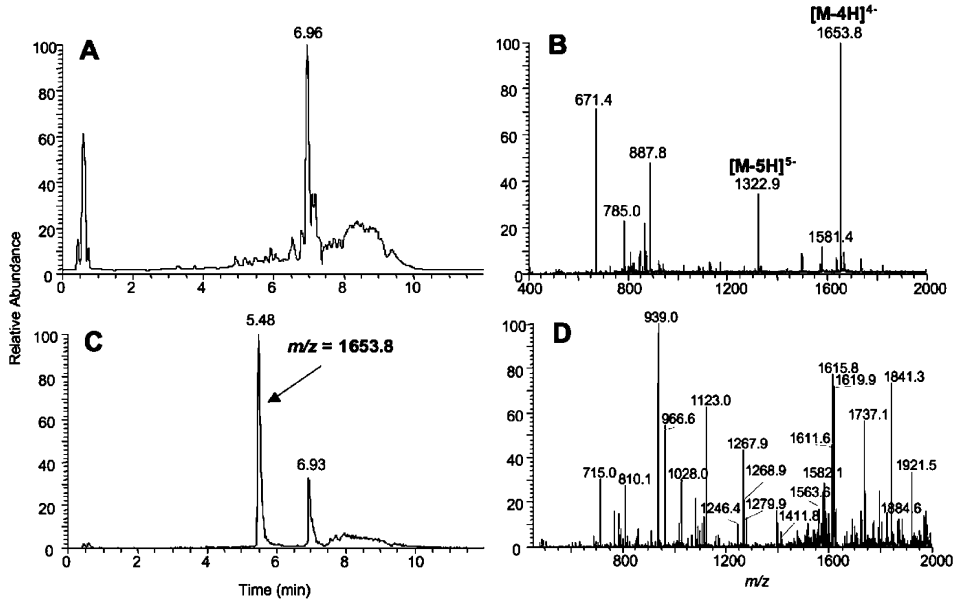

FIGURE 5: LC−MS analysis of the MP via detection of the DNA−hAGT cross-link. hAGT was incubated with CJW98 (200 pmol) in AGT reaction buffer for 3 h at 37 °C. The reaction mixture was then separated via SDS−PAGE using a 20% gel. Bands corresponding to the DNA−hAGT cross-links were excised, digested with trypsin, and analyzed: (A) total ion chromatogram (TIC) of the trypsin-digested band (median product), (B) ESI mass spectrum of the products eluting at ~5.48 min [peaks at *m/z* 1653.8 and 1322.9 correspond to the −4 and −5 charged species of the CJW98−hAGT(peptide) product, respectively], (C) chromatogram of the *m/z* 1653.8 species, and (D) CID mass spectrum of the *m/z* 1653.8 species.

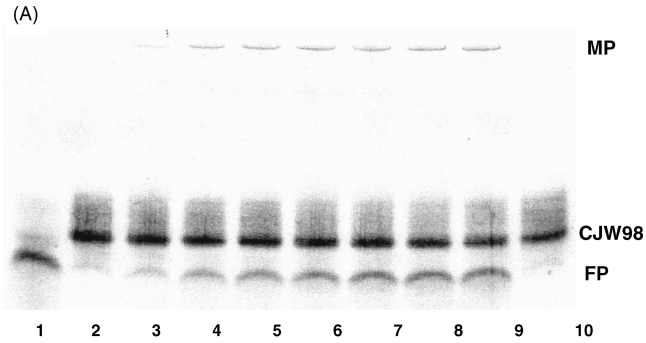

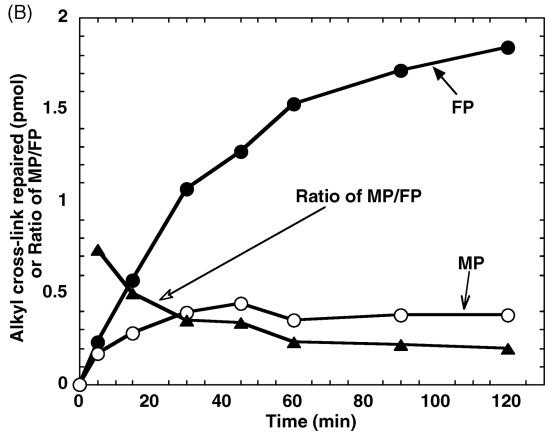

FIGURE 6: Time course of repair of 17-mer seven-carbon cross-linked oligo CJW98 by hAGT. (A) The products were separated by denaturing PAGE: lane 1, 4 pmol of 98-C and 45 pmol of hAGT; lanes 2−9, 4 pmol of CJW98 incubated with 45 pmol of hAGT for 0, 5, 15, 30, 45, 60, 90, and 120 min, respectively; lane 10, 4 pmol of CJW98 incubated with 45 pmol of C145S for 120 min. (B) The amount of products was determined with ImageQuant, and the amount of product formed is shown: MP, hAGT−DNA complex (○); FP, free 17-mer oligo (●); MP:FP ratio (▲).

oligos with a seven-carbon cross-link, a four-carbon alkyl interstrand cross-link [CJW119 (Figure 1)] was repaired by

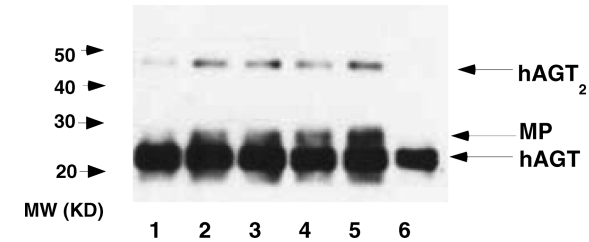

FIGURE 7: Formation of the hAGT dimer after incubation with CJW98. hAGT was incubated with CJW98 for 2 h at 37 °C in 15 μL of reaction buffer. The samples were then separated by SDS−PAGE using 15% gels, and AGT protein was detected using antiserum ATO-1: lanes 1−5, 1, 2, 3, 4, and 5 pmol of CJW98, respectively, and 10 pmol of hAGT; lane 6, 5 pmol of hAGT. MP is the hAGT−DNA complex. Similar results (not shown) were observed using anti-Penta His antibody for detection.

hAGT very poorly (Figure 8). A very small amount of covalent hAGT−DNA complex and of the free oligo product could be detected; however, the ratio of MP to FP was close to 1, and no hAGT dimer could be detected on Western blots (results not shown). Therefore, it appears that the hAGT is only very weakly active in attacking the four-carbon alkyl interstrand cross-link and is totally unable to repair the hAGT−oligo complex when this is linked to the guanine-O^6 by a short four-carbon linker.

Model of Alkyl Interstrand Cross-Link Repair by hAGT. To understand differences in the ability of hAGT to repair alkyl interstrand cross-link substrates with four- and seven-carbon linkers, we modeled the resulting hAGT−DNA complex and hAGT dimer products (Figure 9). Coordinates for these models are given in Supporting Information Tables S2 and S3. These models reveal several insights into alkyl interstrand cross-link repair by hAGT. In the hAGT−DNA complex models, the guanine targeted for repair is rotated into the active site and the associated carbon linkers are nestled in the active site channel (Figure 9A), which is lined with Glu30, Ile31, Lys32, Leu33, Tyr114, Met134, Arg135,

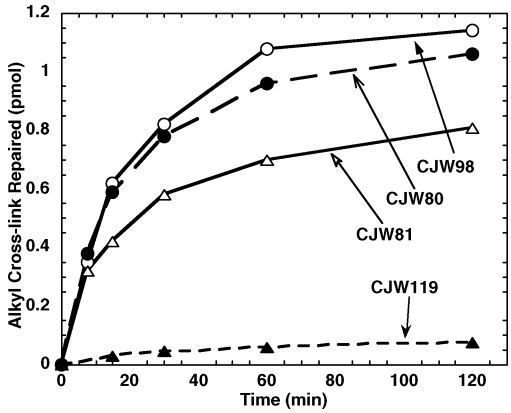

FIGURE 8: Relative rates of repair of CJW80, CJW81, CJW98, and 11-mer four-carbon cross-linked oligo CJW119 by hAGT. Two picomoles of each substrate was incubated with 30 pmol of hAGT for the time shown. The samples were separated by denaturing PAGE, and the products were identified as described in Experimental Procedures. The repairs of CJW98 (○), CJW80 (●), CJW81 (△), and CJW119 (▲) are shown.

Gly136, Asn137, Pro138, Pro140, Ser145, Val148, Asn157, Tyr158, Ser159, Gly160, and Lys165. The seven-carbon linker spans the entire length of the channel, placing the nontarget guanine on the exterior of the protein. In contrast, this nontarget guanine is mostly buried in the active site channel with the shorter four-carbon linker, thereby hindering it from adopting a suitable conformation for its subsequent repair by a second AGT molecule. In agreement with these observations, an AGT C-terminal domain dimer linked at Cys145 by a seven-carbon linker, but not a four-carbon linker, can reasonably be modeled (Figure 9B). The short four-carbon linker results in dimer protein−protein steric clash, which explains why this product is not observed experimentally. Finally, in models for both substrates, the DNA duplex would have to be forced apart locally to repair the target guanine (Figure 9C). Thus, repair of these cross-links by AGT likely disrupts the DNA double helix.

Repair of an Alkyl Interstrand Cross-Link with Seven Carbons by hAGT Mutants and E. coli AGTs. A number of mutants of hAGT with alterations in the active site were examined for the ability to repair the cross-linked oligo substrates. In many cases, the repair was too slow for accurate measurement of the rate of repair. Therefore, the results, which are listed in Table 2, are expressed as the amount of protein needed to obtain 25% repair in the standard assay for either methylated DNA or the cross-linked oligos. As indicated in the footnote of Table 2, the values for 25% repair of methylated DNA by each of the proteins tested do reflect the rate constant for repair of O^6-methylguanine by these proteins.

Arg128 is postulated as the residue that replaces the target nucleotide when this is flipped from DNA into the active site pocket by hAGT binding (*4, 15, 16*). Replacement of this Arg with Lys reduces the rate of repair of methylated DNA slightly as previously reported (*15, 28*) but actually increased the rate of cross-link repair by ~2-fold (Table 2). Replacement of this residue with Ala or Gly, which profoundly reduced the rate of repair of methylated DNA in agreement with published studies (*15, 28*), also reduced the rate of repair of cross-links to an approximately similar degree. The results are compatible with the model shown in Figure 9C. Arg128 is presumably needed to open the duplex to start the repair reaction, and since Arg128 stabilizes the open duplex for repair, the faster R128K repair rate suggests a faster off rate for this mutant.

Tyr114 is thought to play a dual role in the repair of methylated DNA by hAGT. Interaction of the target nucleotide with the aromatic side chain causes rotation of the nucleotide phosphate bond which is key for the flipping, and its OH group then interacts with N3 of the target guanine to facilitate the alkyl transfer (*4, 15, 16, 19*). Therefore, alteration of Tyr114 to Phe, which affects only the latter, reduces the rate constant for methyl repair by ~30-fold, but alteration to Ala has a much greater effect (~600-fold) as previously published (*30*). However, both of these mutations greatly reduced the rate of repair of cross-links (Table 2). One possible explanation for this decreased activity of the Phe and Ala mutants for cross-link repair is that both lack the Tyr114 OH hydrogen bond with the damaged guanine N3 atom, which likely serves to position alkyl-O^6-guanine and lower its negative charge. The absence of this hydrogen bond could result in a slightly different distance from the alkyl group to Cys145, which could lead to a decreased repair rate. This effect would likely be more pronounced for alkyl interstrand cross-link substrates since the damage is large in size. In support of this idea, the distance from the Tyr114 OH group to guanine N3 is ~2.5 Å for methylguanine in PDB entry 1t38 and ~2.9 Å for four- and seven-carbon cross-link substrate models (Figure 9), and the distance from the Cys145 SH group to alkyl damage C1 is 2.7, 3.6, and 3.9 Å for O^6-methylguanine, four-carbon cross-link, and seven-carbon cross-link substrates, respectively. Another possible explanation for decreased mutant activity is that steric effects of large cross-link substrates result in their limited conformational flexibility, which could prevent the alkyl group from easily adopting an orientation amenable to repair. Longer alkyl groups are repaired less efficiently than shorter ones by hAGT (*7*), and this effect may be greatly enhanced when combined with Tyr114 mutants.

Several mutations at the active site for hAGT greatly weaken the ability to react with the low-MW pseudosubstrate drugs O^6-benzylguanine (*42*−*44*) and O^6-(4-bromothenyl)guanine (*45*) but have only a modest effect on the ability to repair methylated DNA. Three of these mutations, G160R (a naturally occurring polymorphic variant) and P140K and Y156H (which were discovered in a screen for O^6-benzylguanine resistant mutants), were tested for the ability to repair cross-links. The rate of repair by G160R was reduced only slightly and to the same extent as the rate of repair of methylated DNA, but no repair of cross-links was detected by mutants P140K and Y156H (Table 2). It is likely that this is due to restrictions in the space available and flexibility of the active site.

This interpretation is consistent with the finding that neither of the *E. coli* AGTs tested, Ogt and Ada-C, was able to repair O^6-G-alkyl-O^6-G cross-links. These *E. coli* repair proteins are also resistant to O^6-benzylguanine (*46*−*48*). Full details of the structure of the Ogt active site are not available, but the Ada-C crystal structure is known (*49*). The Ada-C active site channel is partially blocked by side chains of bulky residues Arg and Trp (corresponding residues in hAGT are Ser and Gly, respectively) and, thus, is unable to accommodate the cross-link, as shown in Figure 9D.

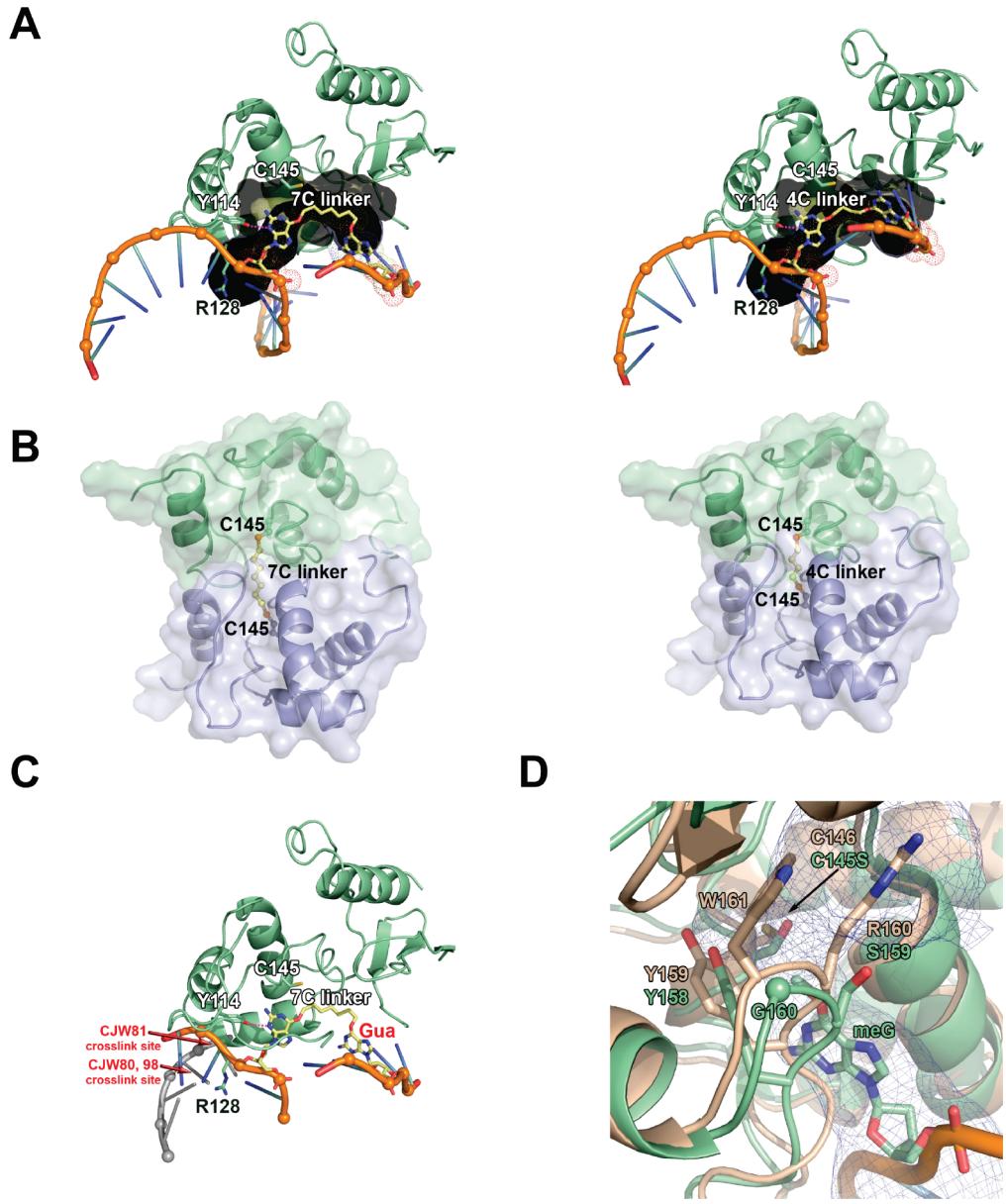

FIGURE 9: Model of O^6-G-alkyl-O^6-G interstrand cross-link repair by AGT. (A) Seven-carbon (left) and four-carbon (right) cross-linked substrate (yellow) modeled within the AGT active site channel (gray). (B) Model of the AGT−AGT dimer resulting from repair of seven-carbon (left) and four-carbon (right) cross-linked substrates. The protein−protein steric clash in the four-carbon model could explain why this product is not observed experimentally. The N-terminal domain of AGT has been omitted from these models. (C) Model of AGT bound to a seven-carbon cross-linked substrate and dsDNA, showing that repair of these cross-links by AGT likely disrupts the DNA double helix. The guanine labeled in red would have to be positioned at one of the cross-link sites (labeled in red) to maintain dsDNA. For clarity, helix 8 is not shown. (D) Ada-C structure (tan; PDB entry 1sfe) overlaid with AGT bound to DNA containing O^6-methylguanine structure (green; PDB entry 1t38). The AGT active site channel is shown as a blue mesh.

DISCUSSION

It is well established that hAGT can prevent interstrand cross-link formation after exposure to chloroethylating agents, but this effect is due to the facile repair of the precursors O^6-(2-chloroethyl)guanine (*50, 51*) or 1,O^6-ethanoguanine (*14*). Our results provide the first evidence that hAGT can actually directly break DNA interstrand cross-links if these involve attachment to the guanine O^6-position. Although we have only demonstrated such reaction with an O^6-O^6 cross-link, it is very likely that a similar transfer would occur with any other cross-link in which one side involves the guanine O^6 recognized by hAGT. However, efficient reaction with hAGT requires that the cross-link be long enough to ensure that the structural alteration of the DNA substrate brought about by hAGT binding, which is needed to place the thiolate anion at Cys145 in the proximity of the CH_2 group attached to the guanine O^6, can take place. The seven-carbon linker is clearly long enough for this even when the two linked bases were offset by one nucleotide and not directly opposite, but the four-carbon linker is too short.

These experimental observations are entirely compatible with the modeling shown in Figure 9C which is based on the crystal structure of hAGT bound to DNA and the mechanism for alkyl transfer proposed on the basis of this structure (*4, 16*). A recent paper providing theoretical simulations from pairwise potentials suggested the possibility of slightly revised roles for Tyr114 and Arg128 in a two-

Table 2: Repair of O^6-Methylguanine and O^6-G-Alkyl-O^6-G Interstrand Cross-Links by hAGT Mutants and Bacterial AGTs[a]

	amount of protein needed for 25% removal of the DNA adduct (pmol)		
		interstrand cross-linked oligo substrate	
protein	methylated DNA substrate	CJW80	CJW81
hAGT[b]	0.08	2.2	4.6
R128K[b]	0.12	1.6	1.8
R128A[b]	62	65	not tested
R128G[b]	91	140	86
Y114F[b]	0.84	>200	>200
Y114A[b]	90	no reaction	no reaction
Ogt	0.08	no reaction	no reaction
Ada-C	0.08	no reaction	no reaction
P140K	1.20	>200	>200
Y158H	1.30	>200	>200
G160R	0.18	5.4	9.6

[a] The values are the means of two or three experiments. [b] The rate constants for repair of O^6-methylguanine in methylated DNA were measured for these proteins: 7×10^7 M^{-1} min^{-1} for wild-type hAGT, 4.3×10^7 M^{-1} min^{-1} for R128K, 0.0007×10^7 M^{-1} min^{-1} for R128A, 0.0004×10^7 M^{-1} min^{-1} for R128G, 0.39×10^7 M^{-1} min^{-1} for Y114F, and 0.0006×10^7 M^{-1} min^{-1} for Y114A.

step kinetic process for lesion recognition by AGT (*19*). Our results are also consistent with this mechanism.

It is noteworthy that the AGTs from *E. coli*, Ada-C and Ogt, were unable to carry out the repair of the O^6-O^6 cross-link even when it did contain the seven-carbon bridge. Modeling based on the Ada-C structure and DNA binding domain (*49, 52*) shown in Figure 9D shows that the limited space in the active site of Ada-C cannot accommodate the cross-link. This steric restriction also accounts for the inability of Ada-C to react with the pseudosubstrate inhibitor O^6-benzylguanine (*15, 47*). The structure of Ogt is not known; however, this protein also reacts very poorly with O^6-benzylguanine (*47*), and its active site is also likely to be more restricted than hAGT. The correlation with the inability to react with O^6-benzylguanine is also seen with the P140K and Y156H mutants of hAGT (*42, 43*), whereas the G160R variant, which is much less resistant to this inhibitor, was able to repair the cross-link (*44*). Busulfan, a strongly cytotoxic immunosuppressive drug, which has been used for preparation for bone marrow transplantation (*24*) and for the treatment of tumors, particularly chronic myelogenous leukemia (*25*), forms a variety of DNA adducts causing mutations, sister chromatid exchanges, and cell death (*53*−*55*). The presence of an unrepaired interstrand cross-link during S phase is likely to be highly toxic to mammalian cells. Although such an O^6-O^6 cross-link might be expected to occur to only a limited extent in cells treated with busulfan, this minor adduct could still contribute significantly to its cell killing ability. It was reported that the toxicity of busulfan was not affected by the activity of hAGT in a cultured human erythromegakaryocytic cell line (LAMA-84) and normal human bone marrow cells in culture (*56*). This is consistent with our finding that the short four-carbon O^6-O^6 cross-link that could be derived from busulfan cannot be repaired by AGT. The inability to repair such cross-links may contribute to the potent immunosuppressive effects of busulfan. In contrast, similar agents producing longer cross-links such as hepsulfam (*24, 57*−*59*), which could form longer seven-carbon O^6-O^6 cross-links, are more likely to be affected by hAGT status. Since hAGT is expressed in a wide variety of human tumors, this could explain their disappointing lack of activity despite initial promise when tested in comparison to busulfan (*25, 59, 60*). If this is the case, their combination with hAGT inactivators such as O^6-benzylguanine or O^6-(4-bromothenyl)guanine may restore utility.

The initial reaction of hAGT with the seven-carbon O^6-O^6 cross-linked substrate forms an hAGT−oligo cross-link in which a guanine-O^6 is linked to Cys145 of hAGT by a seven-carbon bridge. The structure of this DNA−protein cross-link was confirmed by LC−MS analysis as shown in Figure 5. On the basis of studies in which hAGT−DNA cross-links are formed by reactions of bis-electrophiles such as dibromomethane (*61*), DBE (*34*), butadiene diepoxide (*62, 63*), and nitrogen mustards (*64*), it is likely that such a protein−DNA cross-link would be both cytotoxic and mutagenic. However, these hAGT−DNA adducts are linked at positions such as the guanine N7 and N^2 atoms, whereas the protein adduct formed in the repair of the O^6-O^6 cross-linked substrate described in this paper is linked at the guanine-O^6. Therefore, it can also be repaired by a second molecule of hAGT as shown in Figures 2, 4, and 6. This repair, which generates an inactive hAGT dimer and restores the DNA structure, would prevent any toxicity. The remarkable ability of the hAGT to accommodate a large substrate such as a hAGT−DNA protein cross-link in its active site pocket is also predictable from the modeling studies shown in Figure 9B. The seven-carbon linker is long enough to allow for the guanine adduct to be placed in the active site pocket in the proximity of the Cys145 acceptor site with the covalently attached hAGT protein sufficiently distant that there is no steric clash between the protein molecules. This displacement could not occur with the four-carbon linker, so the very slow reaction that occurs with this O^6-O^6 substrate stops at the formation of the hAGT−oligo complex.

In summary, our results add to the spectrum of adducts that are repaired by hAGT. This direct repair reaction requires the attachment of the adduct to the O^6-position (*5*−*7*), but short alkyl adducts such as methyl and ethyl (*65*), longer linear adducts such as *n*-propyl, *n*-butyl, and 2-chloroethyl (*50, 51, 66*), bulky adducts such as benzyl (*7, 18*) and pyridyloxobutyl (*7, 67*), cyclic intermediates such as N^1,O^6-ethanoxanthine (*68*) and 1,O^6-ethanoguanine (*14*), and, as shown here, DNA interstrand cross-links can be repaired.

SUPPORTING INFORMATION AVAILABLE

LC−MS analysis of the 17-mer−AGT complex and coordinates for models of AGT with four-carbon and seven-carbon O^6-G-alkyl-O^6-G interstrand cross-links. This material is available free of charge via the Internet at http://pubs.acs.org.

REFERENCES

1. Pegg, A. E. (2000) Repair of O^6-alkylguanine by alkyltransferases. *Mutat. Res. 462*, 83–100.
2. Margison, G. P., and Santibáñez-Koref, M. F. (2002) O^6-Alkylguanine-DNA alkyltransferase: Role in carcinogenesis and chemotherapy. *BioEssays 24*, 255–266.
3. Margison, G., Povey, A. C., Kaina, B., and Santibáñez-Koref, M. F. (2003) Variability and regulation of O^6-alkylguanine-DNA alkyltransferase. *Carcinogenesis 24*, 625–635.
4. Tubbs, J. L., Pegg, A. E., and Tainer, J. A. (2007) DNA binding, nucleotide flipping, and the helix-turn-helix motif in base repair

by O^6-alkylguanine-DNA alkyltransferase and its implications for cancer chemotherapy. *DNA Repair 6*, 1100–1115.
5. Pegg, A. E., Dolan, M. E., and Moschel, R. C. (1995) Structure, function and inhibition of O^6-alkylguanine-DNA alkyltransferase. *Prog. Nucleic Acids Res. Mol. Biol. 51*, 167–223.
6. Mijal, R. S., Kanugula, S., Vu, C. C., Fang, Q., Pegg, A. E., and Peterson, L. A. (2006) DNA sequence context affects repair of the tobacco-specific adduct O^6-[4-oxo-4-(3-pyridyl)butyl]guanine by human O^6-alkylguanine-DNA alkyltransferases. *Cancer Res. 66*, 4968–4974.
7. Coulter, R., Blandino, M., Tomlinson, J. M., Pauly, G. T., Krajewska, M., Moschel, R. C., Peterson, L. A., Pegg, A. E., and Spratt, T. E. (2007) Differences in the rate of repair of O^6-alkylguanines in different sequence contexts by O^6-alkylguanine-DNA alkyltransferase. *Chem. Res. Toxicol. 20*, 1966–1971.
8. Gerson, S. L. (2002) Clinical relevance of *MGMT* in the treatment of cancer. *J. Clin. Oncol. 20*, 2388–2399.
9. Erickson, L. C., Laurent, G., Sharkey, N. A., and Kohn, K. W. (1980) DNA cross-linking and monoadduct repair in nitrosourea-treated human tumor cells. *Nature 288*, 727–729.
10. Erickson, L. C., Bradley, M. O., Ducore, J. M., Ewig, R. A., and Kohn, K. W. (1980) DNA cross-linking and cytotoxicity in normal and transformed human cells treated with antitumor nitrosoureas. *Proc. Natl. Acad. Sci. U.S.A. 77*, 467–471.
11. Ludlum, D. B. (1997) The chloroethylnitrosoureas: Sensitivity and resistance to cancer chemotherapy at the molecular level. *Cancer Invest. 15*, 588–598.
12. Bodell, W. J., Tokuda, K., and Ludlum, D. B. (1988) Differences in DNA alkylation products formed in sensitive and resistant human glioma cells treated with N-(2-chloroethyl)-N-nitrosourea. *Cancer Res. 48*, 4489–4492.
13. Gonzaga, P. E., Harris, L., Margison, G. P., and Brent, T. P. (1990) Evidence that covalent complex formation between BCNU-treated oligonucleotides and *E. coli* alkyltransferases requires the O^6-alkylguanine function. *Nucleic Acids Res. 18*, 3961–3966.
14. Gonzaga, P. E., Potter, P. M., Niu, T., Yu, D., Ludlum, D. B., Rafferty, J. A., Margison, G. P., and Brent, T. P. (1992) Identification of the cross-link between human O^6-methylguanine-DNA methyltransferase and chloroethylnitrosourea-treated DNA. *Cancer Res. 52*, 6052–6058.
15. Daniels, D. S., Mol, C. D., Arvai, A. S., Kanugula, S., Pegg, A. E., and Tainer, J. A. (2000) Active and alkylated human AGT structures: A novel zinc site, inhibitor and extrahelical binding. DNA damage reversal revealed by mutants and structures of active and alkylated human AGT. *EMBO J. 19*, 1719–1730.
16. Daniels, D. S., Woo, T. T., Luu, K. X., Noll, D. M., Clarke, N. D., Pegg, A. E., and Tainer, J. A. (2004) Novel modes of DNA binding and nucleotide flipping by the human DNA repair protein AGT. *Nat. Struct. Mol. Biol. 11*, 714–720.
17. Duguid, E. M., Rice, P. A., and He, C. (2005) The structure of the human AGT protein bound to DNA and its implications for damage detection. *J. Mol. Biol. 350*, 657–666.
18. Zang, H., Fang, Q., Pegg, A. E., and Guengerich, F. P. (2005) Kinetic analysis of steps in the repair of damaged DNA by human O^6-alkylguanine DNA-alkyltransferase. *J. Biol. Chem. 280*, 30873–30881.
19. Hu, J., Ma, A., and Dinner, A. R. (2008) A two-step nucleotide-flipping mechanism enables kinetic discrimination of DNA lesions by AGT. *Proc. Natl. Acad. Sci. U.S.A. 105*, 4615–4620.
20. Guengerich, F. P., Fang, Q., Liu, L., Hachey, D. L., and Pegg, A. E. (2003) O^6-Alkylguanine-DNA alkyltransferase: Low pK_a and reactivity of cysteine 145. *Biochemistry 42*, 10965–10970.
21. Wibley, J. E. A., Pegg, A. E., and Moody, P. C. E. (2000) Crystal structure of the human O^6-alkylguanine-DNA alkyltransferase. *Nucleic Acids Res. 28*, 393–401.
22. Hashimoto, H., Inoue, T., Nishioka, M., Fujiwara, S., Takagi, M., Imanaka, T., and Kai, Y. (1999) Hyperthermostable protein structure maintained by intra- and inter-helix ion pairs in archael O^6-methylguanine-DNA methyltransferase. *J. Mol. Biol. 292*, 707–716.
23. Roberts, A., Pelton, J. G., and Wemmer, D. E. (2006) Structural studies of MJ1529, an O^6-methylguanine-DNA methyltransferase. *Magn. Reson. Chem. 44* (Spec. No.), S71–S82.
24. Westerhof, G. R., Ploemacher, R. E., Boudewijn, A., Blokland, I., Dillingh, J. H., McGown, A. T., Hadfield, J. A., Dawson, M. J., and Down, J. D. (2000) Comparison of different busulfan analogues for depletion of hematopoietic stem cells and promotion of donor-type chimerism in murine bone marrow transplant recipients. *Cancer Res. 60*, 5470–5478.
25. Berger, D. P., Winterhalter, B. R., Dengler, W. A., and Fiebig, H. H. (1992) Preclinical activity of hepsulfam and busulfan in solid human tumor xenografts and human bone marrow. *Anticancer Drugs 3*, 531–539.
26. Nallamsetty, S., Kapust, R. B., Tozser, J., Cherry, S., Tropea, J. E., Copeland, T. D., and Waugh, D. S. (2004) Efficient site-specific processing of fusion proteins by tobacco vein mottling virus protease in vivo and in vitro. *Protein Expression Purif. 38*, 108–115.
27. Wilds, C. J., Booth, J. D., and Noronha, A. M. (2006) Synthesis of oligonucleotides containing an O^6-G-alkyl-O^6-G interstrand cross-link. *Tetrahedron Lett. 47*, 9125–9128.
28. Kanugula, S., Goodtzova, K., Edara, S., and Pegg, A. E. (1995) Alteration of arginine-128 to alanine abolishes the ability of human O^6-alkylguanine-DNA alkyltransferase to repair methylated DNA but has no effect on its reaction with O^6-benzylguanine. *Biochemistry 34*, 7113–7119.
29. Liu, L., Xu-Welliver, M., Kanugula, S., and Pegg, A. E. (2002) Inactivation and degradation of O^6-alkylguanine-DNA alkyltransferase after reaction with nitric oxide. *Cancer Res. 62*, 3037–3043.
30. Goodtzova, K., Kanugula, S., Edara, S., and Pegg, A. E. (1998) Investigation of the role of tyrosine-114 in the activity of human O^6-alkylguanine-DNA alkyltransferase. *Biochemistry 37*, 12489–12495.
31. Fang, Q., Kanugula, S., and Pegg, A. E. (2005) Function of domains of human O^6-alkylguanine-DNA alkyltransferase. *Biochemistry 44*, 15396–15405.
32. Fang, Q., Loktionova, N. A., Moschel, R. C., Javanmard, S., Pauly, G. T., and Pegg, A. E. (2008) Differential inactivation of polymorphic variants of human O^6-alkylguanine-DNA alkyltransferase. *Biochem. Pharmacol. 75*, 618–626.
33. Maniatis, T., Fritsch, E. F., and Sambrook, J. (1982) *Molecular Cloning*, Cold Spring Harbor Laboratory Press, New York.
34. Liu, L., Pegg, A. E., Williams, K. M., and Guengerich, F. P. (2002) Paradoxical enhancement of the toxicity of 1,2-dibromoethane byO^6-alkylguanine-DNA alkyltransferase. *J. Biol. Chem. 277*, 37920–37928.
35. Pegg, A. E., Wiest, L., Mummert, C., and Dolan, M. E. (1991) Production of antibodies to peptide sequences present in human O^6-alkylguanine-DNA alkyltransferase and their use to detect this protein in cell extracts. *Carcinogenesis 12*, 1671–1677.
36. Brunger, A. T., Adams, P. D., Clore, G. M., DeLano, W. L., Gros, P., Grosse-Kunstleve, R. W., Jiang, J. S., Kuszewski, J., Nilges, M., Pannu, N. S., Read, R. J., Rice, L. M., Simonson, T., and Warren, G. L. (1998) Crystallography & NMR system: A new software suite for macromolecular structure determination. *Acta Crystallogr. D54*, 905–921.
37. Brooks, B. R., Bruccoleri, R. E., Olafson, B. D., States, D. J., Swaminathan, S., and Karplus, M. (1983) CHARMM: A program for macromolecular energy, minimization, and dynamics calculations. *J. Comput. Chem. 4*, 1887–1217.
38. MacKerell, A. D., Brooks, B. P., Brooks, I. C. L., Nilsson, L., Roux, B., Won, Y., and Karplus, M. (1998) CHARMM: The energy function and its parameterization with an overview of the program. In *The Encyclopedia of Computational Chemistry* (Schleyer, P. V. R. e. a. Ed.) pp 271−277, John Wiley & Sons, Chichester, U.K.
39. Dundas, J., Ouyang, Z., Tseng, J., Binkowski, A., Turpaz, Y., and Liang, J. (2006) CASTp: Computed atlas of surface topography of proteins with structural and topographical mapping of functionally annotated residues. *Nucleic Acids Res. 34*, W116–W118.
40. Petrek, M., Kosinova, P., Koca, J., and Otyepka, M. (2007) MOLE: A Voronoi diagram-based explorer of molecular channels, pores, and tunnels. *Structure 15*, 1357–1363.
41. Liu, L., Hachey, D. L., Valadez, G., Williams, K. M., Guengerich, F. P., Loktionova, N. A., Kanugula, S., and Pegg, A. E. (2004) Characterization of a mutagenic DNA adduct formed from 1,2-dibromoethane by O^6-alkylguanine-DNA alkyltransferase. *J. Biol. Chem. 279*, 4250–4259.
42. Xu-Welliver, M., Kanugula, S., and Pegg, A. E. (1998) Isolation of human O^6-alkylguanine-DNA alkyltransferase mutants highly resistant to inactivation by O^6-benzylguanine. *Cancer Res. 58*, 1936–1945.
43. Xu-Welliver, M., Leitao, J., Kanugula, S., and Pegg, A. E. (1999) Alteration of the conserved residue tyrosine-158 to histidine renders human O^6-alkylguanine-DNA alkyltransferase insensitive to the inhibitor O^6-benzylguanine. *Cancer Res. 59*, 1514–1519.
44. Xu-Welliver, M., Leitao, J., Kanugula, S., Meehan, W. J., and Pegg, A. E. (1999) The role of codon 160 in sensitivity of human O^6-

alkylguanine-DNA alkyltransferase to O^6-benzylguanine. *Biochem. Pharmacol. 58*, 1279–1285.
45. Woolford, L. B., Southgate, T. D., Margison, G. P., Milsom, M. D., and Fairbairn, L. J. (2006) The P140K mutant of human O^6-methylguanine-DNA-methyltransferase (MGMT) confers resistance in vitro and in vivo to Temozolomide in combination with the novel MGMT inactivator O^6-(4-bromothenyl)guanine. *J. Gene Med. 8*, 29–34.
46. Dolan, M. E., Pegg, A. E., Dumenco, L. L., Moschel, R. C., and Gerson, S. L. (1991) Comparison of the inactivation of mammalian and bacterial O^6-alkylguanine-DNA alkyltransferases by O^6-benzylguanine. *Carcinogenesis 12*, 2305–2310.
47. Pegg, A. E., Boosalis, M., Samson, L., Moschel, R. C., Byers, T. L., Swenn, K., and Dolan, M. E. (1993) Mechanism of inactivation of human O^6-alkylguanine-DNA alkyltransferase by O^6-benzylguanine. *Biochemistry 32*, 11998–12006.
48. Elder, R. H., Margison, G. P., and Rafferty, J. A. (1994) Differential inactivation of mammalian and *E. coli* O^6-alkylguanine-DNA alkyltransferase by O^6-benzylguanine. *Biochem. J. 298*, 231–235.
49. Moore, M. H., Gulbus, J. M., Dodson, E. J., Demple, B., and Moody, P. C. E. (1994) Crystal structure of a suicidal DNA repair protein: The Ada O^6-methylguanine-DNA methyltransferase from *E. coli*. *EMBO J. 13*, 1495–1501.
50. Gibson, N., Zlotogorski, C., and Erickson, L. C. (1985) Specific DNA repair mechanisms may protect some human tumor cells from DNA interstrand crosslinking by chloroethylnitrosoureas but not from crosslinking by other anti-tumor alkylating agents. *Carcinogenesis 6*, 445–450.
51. Brent, T. P. (1986) Inactivation of purified human O^6-alkylguanine-DNA alkyltransferase by alkylating agents or alkylated DNA. *Cancer Res. 46*, 2320–2323.
52. Verdemato, P. E., Brannigan, J. A., Dambion, C., Zuccotto, F., Moody, P. C. E., and Lian, L.-Y. (2000) DNA-binding mechanism of the *Escherichia coli* Ada O^6-alkylguanine-DNA alkyltransferase. *Nucleic Acids Res. 28*, 3710–3718.
53. Sanderson, B. J., and Shield, A. J. (1996) Mutagenic damage to mammalian cells by therapeutic alkylating agents. *Mutat. Res. 355*, 41–57.
54. Tong, W. P., and Ludlum, D. B. (1980) Crosslinking of DNA by busulfan. Formation of diguanyl derivatives. *Biochim. Biophys. Acta 608*, 174–181.
55. Morales-Ramirez, P., and Gonzalez-Beltran, F. (2007) Different behavior of SCE-eliciting lesions induced by low and high doses of busulfan. *Environ. Mol. Mutagen. 48*, 706–714.
56. Westerhof, G. R., Down, J. D., Blokland, I., Wood, M., Boudewijn, A., Watson, A. J., McGown, A. T., Ploemacher, R. E., and Margison, G. P. (2001) O^6-Benzylguanine potentiates BCNU but not busulfan toxicity in hematopoietic stem cells. *Exp. Hematol. 29*, 633–638.
57. Sanyal, U., Nanda, R., Samanta, S., Pain, A., Dutta, S., Verma, A. S., Rider, B. J., and Agrawal, K. C. (2000) Evaluation of dimethylaminosulfonates of alkane diols as a novel group of anticancer agents. *Cancer Lett. 155*, 89–97.
58. Pacheco, D. Y., Stratton, N. K., and Gibson, N. W. (1989) Comparison of the mechanism of action of busulfan with hepsulfam, a new antileukemic agent, in the L1210 cell line. *Cancer Res. 49*, 5108–5110.
59. Streeper, R. T., Cotter, R. J., Colvin, M. E., Hilton, J., and Colvin, O. M. (1995) Molecular pharmacology of hepsulfam, NSC 3296801: Identification of alkylated nucleosides, alkylation site, and site of DNA cross-linking. *Cancer Res. 55*, 1491–1498.
60. Hendricks, C. B., Grochow, L. B., Rowinsky, E. K., Forastiere, A. A., McGuire, W. P., Ettinger, D. S., Sartorius, S., Lubejko, B., and Donehower, R. C. (1991) Phase I and pharmacokinetic study of hepsulfam (NSC 329680). *Cancer Res. 51*, 5781–5785.
61. Liu, L., Williams, K. M., Guengerich, F. P., and Pegg, A. E. (2004) O^6-Alkylguanine-DNA alkyltransferase has opposing effects in modulating the genotoxicity of dibromomethane and bromomethyl acetate. *Chem. Res. Toxicol. 17*, 742–752.
62. Valadez, J. G., Liu, L., Loktionova, N. A., Guengerich, F. P., and Pegg, A. E. (2004) Activation of bis-electrophiles to mutagenic conjugates by human O^6-alkylguanine-DNA alkyltransferase. *Chem. Res. Toxicol. 17*, 972–982.
63. Loeber, R., Rajesh, M., Fang, Q., Pegg, A. E., and Tretyakova, N. (2006) Cross-linking of the human DNA repair protein O^6-alkylguanine DNA alkyltransferase to DNA in the presence of 1,2,3,4-diepoxybutane. *Chem. Res. Toxicol. 19*, 645–654.
64. Loeber, R., Michaelson, E., Fang, Q., Campbell, C., Pegg, A. E., and Tretyakova, N. (2008) Cross-linking of the DNA repair protein O^6-alkylguanine DNA alkyltransferase to DNA in the presence of antitumor nitrogen mustards. *Chem. Res. Toxicol. 21*, 787–795.
65. Pegg, A. E., Scicchitano, D., and Dolan, M. E. (1984) Comparison of the rates of repair of O^6-alkylguanines in DNA by rat liver and bacterial O^6-alkylguanine-DNA alkyltransferase. *Cancer Res. 44*, 3806–3811.
66. Morimoto, K., Dolan, M. E., Scicchitano, D., and Pegg, A. E. (1985) Repair of O^6-propylguanine and O^6-butylguanine in DNA by O^6-alkylguanine-DNA alkyltransferases from rat liver and *E. coli*. *Carcinogenesis 6*, 1027–1031.
67. Wang, L., Spratt, T. E., Liu, X.-L., Hecht, S. S., Pegg, A. E., and Peterson, L. A. (1997) Pyridyloxobutyl adduct O^6-[4-oxo-4-(3-pyridyl)butyl]guanine, is present in 4-(acetoxymethylnitrosamino-1-(3-pyridyl)-1-butanone-treated DNA and is a substrate for O^6-alkylguanine-DNA alkyltransferase. *Chem. Res. Toxicol. 10*, 562–567.
68. Noll, D. M., and Clarke, N. D. (2001) Covalent capture of a human O^6-alkylguanine alkyltransferase-DNA complex using N^1-O^6-ethanoxanthosine, a mechanism-based crosslinker. *Nucleic Acids Res. 29*, 4025–2034.

BI8008664